

Hamidreza Shagholani^{1*} and Sayed Mehdi Ghoreishi²

¹Institute of Nanoscience and Nanotechnology, University of Kashan, Kashan, I.R. Iran

²Department of Analytical Chemistry, Faculty of Chemistry, University of Kashan, Kashan, I.R. Iran

Dates: Received: 15 February, 2017; Accepted: 02 March, 2017; Published: 06 March, 2017

*Corresponding author: Hamidreza Shagholani, Institute of Nanoscience and Nanotechnology, University of Kashan, Kashan, I.R. Iran, Tel: +98 31 55912395; Fax: +98 31 55912397; E-mail: Shagholani.hr@gmail.com

Keywords: Magnetite nanoparticles; Chitosan; Poly (acrylic acid); Albumin; Immunoglobulin G

<https://www.peertechz.com>

Research Article

Synthesis of Nanocomposition of Poly Acrylic Acid/Chitosan Coated-Magnetite Nanoparticles to Investigation of Interaction with BSA and IGG Proteins

Abstract

Among the nanomaterial being applied for treatment and diagnosis field, magnetic NPs especially magnetite phase of iron oxide have been significantly interested due to their natural magnetic properties. In this study, a nanocomposition of poly (acrylic acid) and chitosan with Fe_3O_4 NPs were prepared in order to investigation for drug delivery systems and plasma protein adsorption. Synthesized NPs were studied by various technics including XRD, TEM, SEM, FT-IR, VSM, DLS, zeta potential and AAS. These NPs have superparamagnetic property that is essential for magnetic NPs to applying in body and drug delivery. Plasma protein adsorption is one of the most important issues for failure of nanocarriers function. In this work, BSA and IgG were used as models of proteins to study adsorption of protein onto NPs by UV-Vis spectroscopy method. Adsorption behavior of NPs for each protein was different. PAA- Fe_3O_4 NPs represent the lowest albumin adsorption and can be expected that have lower adsorption of protein in the body. The release profile of ascorbic acid from PAA- Fe_3O_4 NPs represents no sensitivity to pH, and NPs showed approximately same release behavior in pH 7.4 and 5.8.

Introduction

Nanomaterials with special structural and physical properties can be used to improvement of treatment and diagnosis of disease [1]. Among the nanomaterials being applied in this field, magnetic nanoparticles (NPs) especially magnetite phase of iron oxide (Fe_3O_4) has been significantly interested because of their natural magnetic properties [2]. Fe_3O_4 NPs with sizes lower than 20 nm are superparamagnetic and have been potential to be used as targeted drug delivery, hyperthermia, magnetic resonance imaging (MRI), magnetic cell sorting, magnetic targeting and immunoassays. Biocompatible polymers and surfactants have been applied with NPs to achieving these purposes [3].

There are barriers that can limit the role of NPs in the body. This may be happened by obstructing their movement, changing in physical properties of NPs or by produce a negative response from the body to NPs [4]. Interaction between NPs and proteins in biosystems has an important effect on the behavior of NPs [5]. Upon administration, proteins in plasma can attach to NPs leading to recognition by the reticuloendothelial system (RES) or mononuclear phagocyte system (MPS) tissues. This causes to collection of NPs in liver, spleen, and bone [6]. In

addition, activation of immune system and non-targeted interaction are problems that can be happened because of interaction with plasma protein [4]. This attaching of protein onto NPs forms a shell around NPs which is named "protein corona". The physicochemical properties of this shell can influence on biological responses [7]. Therefore, nonspecific interaction with proteins in blood circulation is one of the most important that can limit NPs function in body and finally remove them from blood stream [4]. Grafting poly (ethylene glycol) to nanomaterials is the most applied approach to reduce nonspecific protein adsorption and phagocyte uptake. Influences of nanomaterials properties like size and surface chemistry to adsorption of protein are poorly studied [1]. However, physicochemical features of nanomaterials and how long being in biological mediums can affect the forming of protein corona. Therefore, these influence on biodistribution of nanomaterials and their functions [8].

In this work, Fe_3O_4 NPs were synthesized and then coated by chitosan. Then, chitosan coated NPs reacted with poly (acrylic acid) (PAA). These NPs have positive and negative surface charge respectively. Coating of NPs prevents them from agglomeration or non-specific interaction with cells. Furthermore, chemical groups provided from polymer can be

used to conjugation of biomedical molecules such as drugs and targeting drugs [4]. Chitosan is a biodegradable cationic polysaccharide with good biocompatibility, and low toxicity. PAA is poly anionic with carbocyclic acid groups which have good interaction with amine groups on the chitosan [9].

Here we studied NPs interaction with bovine serum albumin (BSA) and Immunoglobulin G (IgG). Albumin and IgG are the most plentiful proteins in human serum [10], but have a different isoelectric point which can influence on protein adsorption behavior [11]. Thus, these proteins are good choices to plasma protein adsorption. Moreover, other important properties of NPs for applying in drug delivery systems such as magnetic properties, size, shape and surface charge were studied. This nanocomposition showed relatively good characteristic for applying in biological environment.

Experimental

Materials and characterization

Iron (II) chloride tetrahydrate, iron (III) chloride hexahydrate, PAA (2000 MW, 63%), ammonium persulfate, NH₄OH (25 wt %), and bovine serum albumin (BSA) all purchased from Merck. IgG protein (50 mg/mL) have obtained from Kashan University of medical sciences and health services. Chitosan with medium molecular weight (deacetylation $\geq 75\%$) was obtained from Sigma-Aldrich.

Powder X-ray diffraction (XRD) pattern of Fe₃O₄ NPs was performed in a Philips X-ray diffractometer using CuK α radiation ($\lambda = 1.54060 \text{ \AA}$). The diffraction angle (2θ) ranged from 10° to 80°. Transmission electron microscopy (TEM) (Philips EM208S, accelerating voltage of 150 kV) and scanning electron microscopy (SEM) (Hitachi S-4160) were used to study the morphology of NPs. Synthesized NPs and their coating were studied by Fourier transform infrared (FT-IR) spectra using a magna-IR spectrometer 550 Nicolet spectrometer. Samples were prepared by using KBr disk method and spectra were recorded in the range of 400–4000 cm⁻¹. Hydrodynamic size and surface charge were obtained on dispersed NPs in deionized water by sonication using a Malvern- DTS Ver 4.20 at room temperature. Vibrating sample magnetometer (VSM) (Meghnatis Daghigh Kavir Co, Iran) was operated to measuring of magnetic properties of NPs. Iron analysis was performed on a Perkin-Elmer 2380 atomic absorption spectrometer by flame (air/C₂H₂). Protein adsorption was studied by a dual beam UV-Vis spectrophotometer (TU-1901, Purkinje General Instrument, Beijing, China).

Methods

Chitosan modified of Fe₃O₄ NPs were synthesized by our pervious published method with some modification [12]. Firstly, Fe₃O₄ NPs were obtained by coprecipitation of iron chloride salts in alkaline medium under sonication in N₂ atmosphere. Fe₃O₄ NPs were separated by magnet and dried in 45 °C for 24 h. Then, NPs were dispersed and mixed with chitosan solution and stirred at a speed of 700 rpm for 12 h to obtaining of chitosan coated of Fe₃O₄ NPs (Ch-Fe₃O₄).

0.4 gr PAA (60% w/v) was dissolved in 20 mL deionized water. Then, 0.07 gr of dispersed Ch-Fe₃O₄ NPs in water was added to PAA solution. The temperature of solution was reached to 55 °C and remained under stirring for 15 min. Finally, 10 mL of ammonium persulfate solution (3% w/v) was added to mixture. The mixture was stirred for 4 h at a speed of 1000 rpm and in 55 °C. After separation by magnet, the product (PAA-Fe₃O₄) was washed twice with deionized water and dried in room temperature.

AAS was used to determine the amount of polymer coating percent on NPs. Each of NPs was weighted by a precise balance exactly. Then, NPs were dissolved in HCl and maintained for overnight. The NPs diluted to 50 mL by adding deionized water and concentration of iron in each solution was measured by an atomic absorption spectrophotometer. Then, coating percent of NPs were calculated by using calibration curve of Fe solutions.

For evaluation of protein adsorption onto NPs surface, 10 mL of BSA and IGG (1mg/mL) were added to 1 mg of NPs. Firstly, these mixtures sonicated for 1 min and then, kept at 37 °C. After 24 h, NPs were separated by centrifuge from the solution. Non- adsorbed protein was studied by a UV-Vis spectrophotometer.

Drug loading and release behavior of PAA-Fe₃O₄ NPs was studied by using of ascorbic acid as a model of drug. A mixture of ascorbic acid and PAA-Fe₃O₄ NPs (55 % w/w) was prepared and kept for 24 h at room temperature. Then NPs were separated from solution by a magnet. A UV-Vis spectrophotometer was used to determine the amount of reminding ascorbic acid in solution and estimating drug loading in PAA-Fe₃O₄ NPs. Following equations were used to calculating of drug loading contents (Eq.1) and drug entrapment efficiency (Eq.2) of NPs.

$$\text{drug loading contents (\%)} = \frac{\text{weight of drug in NPs}}{\text{weight of prepared NPs}} \times 100 \quad (1)$$

$$\text{drug entrapment efficiency (\%)} = \frac{\text{weight of drug in NPs}}{\text{weight of drug injected}} \times 100 \quad (2)$$

The release profile of ascorbic acid from PAA-Fe₃O₄ NPs was estimated by the dialysis method in phosphate buffered saline (PBS) at 37 °C. 5 mg of drug loaded PAA-Fe₃O₄ NPs and 3 mL PBS buffers were incubated in a dialysis membrane bag (molecular weight cutoff 14 kDa). The dialysis bag was immersed into 100 mL of PBS solution at different pH (7.4 and 5.8). The released of ascorbic acid from PAA-Fe₃O₄ NPs by a UV-Vis spectrophotometer. 3 mL of the sample was sampled at defined time periods for analysis and then, 3 mL of fresh buffer was replaced to the release medium.

Brine shrimp mortality procedure was applied to assessment of NPs toxicity [13,14]. 1 gr Brine shrimp eggs were placed in 1 L salt solution (25 gr/L) at 28 °C. The vessel was under continuous light and air pumping for 48 h. Under these conditions; Brine shrimp eggs were hatched. The toxicity of NPs was tested via brine shrimp mortality at the concentration of 1 $\mu\text{g}/\text{mL}$ NPs over 24 hours. Experiment was performed in test tubes that were cleaned by HCl and acetone previously. In each tube, 10 brine shrimps were placed in 10 mL of NPs dispersion. After 24

h, the live brine shrimps were counted for each tube along with control (without NPs).

Results and Discussion

Ferric and ferrous salts were used for synthesized Fe_3O_4 NPs. The reaction was performed by adding ammonia under sonication and N_2 atmosphere. This procedure is very fast, and the reaction is carried out only in 15 min. The XRD pattern was obtained for Fe_3O_4 NPs (Figure 1) after drying in an oven at 40 °C. The corresponding planes are showed for each peak. These NPs show characteristic peaks at 30.1973° , 35.5022° , 43.1439° , 53.6228° , 57.1545° , 62.7770° that are related to (2 2 0), (3 1 1), (4 0 0), (4 2 2), (5 1 1) and (4 4 0) of reflection plane indices, respectively (Ref. pattern: 01-1111). Therefore, XRD showed that NPs were Fe_3O_4 (magnetite). This indicated that magnetite NPs obtained under sonication have good quality and purity.

For stabilization and functionalization, Fe_3O_4 NPs were coated by chitosan in acetic acid solution (Ch- Fe_3O_4). Then, obtained NPs were reacted with PAA to forming PAA- Fe_3O_4 . Coating with polymers makes NPs stable in aqueous solutions and supplies functional groups at the surface of NPs. These functional groups can be used to conjugating of biomolecules to the NPs [15]. TEM image of NPs are represented in Figure 2. Fe_3O_4 NPs (Figure 2a) showed a monodispersed and spherical shapes. These NPs have an average size about 10 nm. Figure 2b indicates that chitosan was successfully placed at the surface of Fe_3O_4 NPs and a shell of polymer can be observed around the particles. Figures 2c and 2d are related to PAA- Fe_3O_4 NPs. Furthermore, SEM images of these NPs are represented in Figure 2e and Figure 2f as can be seen, these NPs have agglomeration structures that Ch- Fe_3O_4 NPs have dispersed in PAA matrixes. PAA- Fe_3O_4 NPs had a mean diameter size of 51.62 nm with a standard deviation of about 9.4 that was determined from the average of 51 nanoparticles in SEM image.

Hydrodynamic diameter size and zeta potential distributions of PAA- Fe_3O_4 NPs are showed in Figure 3. These NPs have an average diameter size about 96.4 with PDI of 0.47 that is bigger from SEM result. The bigger size obtained from DLS can be related to partial agglomeration [16], and swelling in water [17].

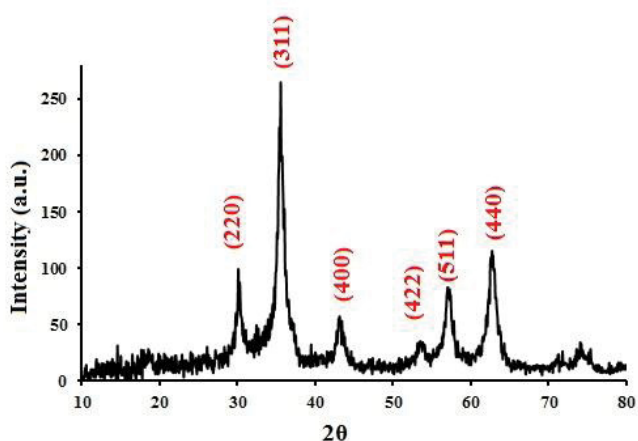


Figure 1: The XRD pattern for Fe_3O_4 NPs.

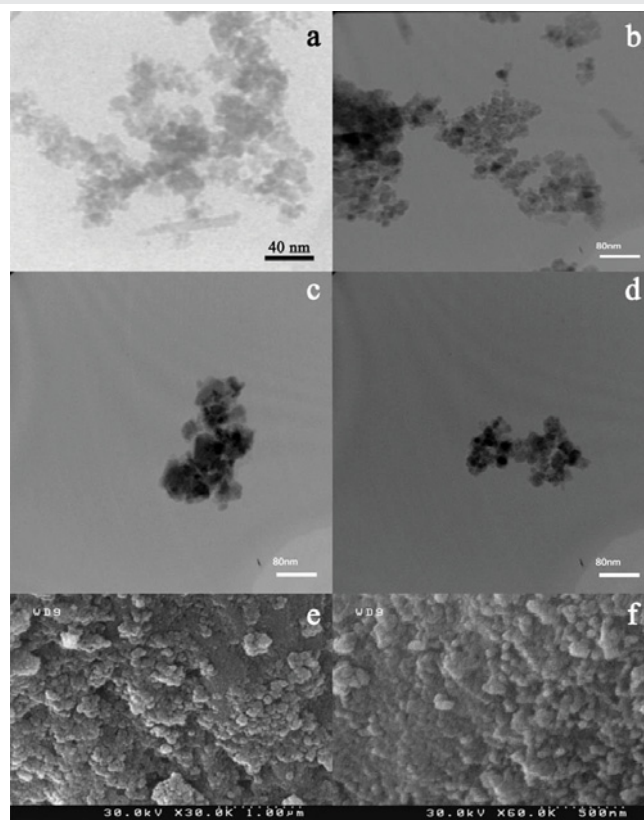


Figure 2: TEM images for a) Fe_3O_4 NPs, b) Ch- Fe_3O_4 NPs, c and d) PAA- Fe_3O_4 NPs and SEM images for PAA- Fe_3O_4 NPs (e and f).

These NPs have an average zeta potential value of -15.6 . This showed that Ch- Fe_3O_4 NPs successfully placed in PAA matrix, and their large positive surface charge [12], turned a relatively smaller negative surface charge. In other words, amine groups at the surface of Ch- Fe_3O_4 NPs have replaced by carbocyclic groups from PAA in PAA- Fe_3O_4 NPs. Hydrodynamic size and surface charge of NPs are important factors for pharmaceutical behavior and their stability in body [4,18]. NPs in colloidal solutions tend to form agglomeration. This agglomeration changes the surface area of NPs that can affect protein binding or cause conformational changes. Polymer coating or using of ultrasonic energy has been used to control of agglomeration [19]. Interaction with cells could be affected by surface charge of NPs. Also, surface charge influences the forming protein corona, and this can influence uptake of NPs. Performing of protein corona reduces adhesion to the cell membrane and internalization efficiency. NPs with positive surface charge can incorporate faster to cells rather than negatively charged ones. Moreover, positive charged NPs have more cytotoxicity potential [20,21].

Charged NPs can also influence on adsorbed protein structure. For example, BSA exposed to positive charged NPs has more changes in comparison of negative charged ones [22].

FT-IR spectroscopy was used to confirm the reaction and characterization of the functional group at the surface of NPs. The FT-IR spectra of obtained products were presented in Figure 4a. The peaks at 631 and 589 cm^{-1} in spectrum of Fe_3O_4 are relating to stretching band of Fe-O in Fe_3O_4 NPs. Also,

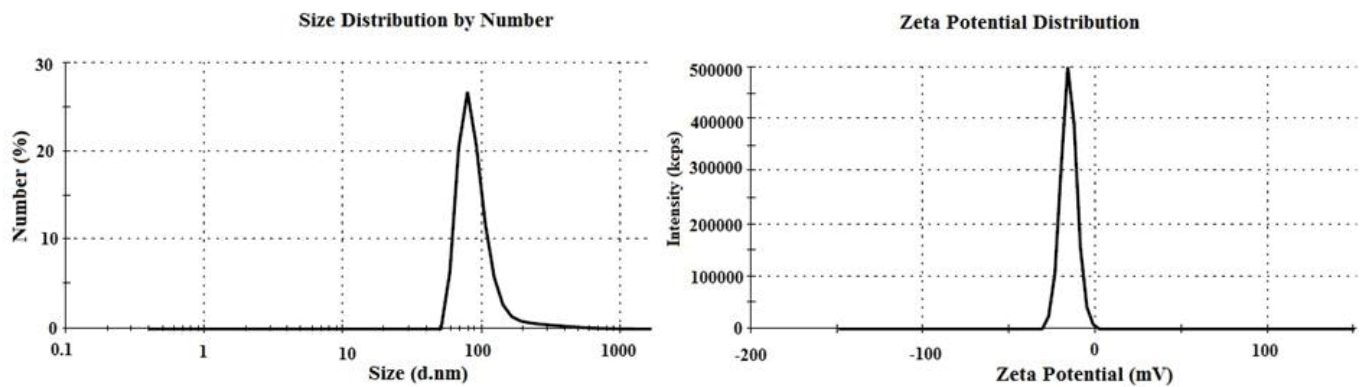


Figure 3: Size and zeta potential distribution of PAA-Fe₃O₄ NPs.

vibration band of OH groups on these NPs caused a broad peak around 3400 cm⁻¹ in the spectrum. Ch-Fe₃O₄ spectrum is related to Fe₃O₄ NPs which coated with chitosan. The absorption band at 1542 cm⁻¹ corresponds to N-H bending vibration. The wide and strong peak between 3100 and 3600 cm⁻¹ relates to stretching vibrations of O-H and N-H bands [12]. In the FT-IR spectrum of PAA-Fe₃O₄ NPs, the peak at 1707 cm⁻¹ showed the stretching mode of the -COOH groups of PAA that placed at the surface of NPs after reaction. Also, the peak at 2923 cm⁻¹ related to the asymmetrical stretching mode of -CH₃ in Figures 2b and c [23]. These results confirm that PAA was successfully placed on the NPs.

Atomic absorption spectroscopy (AAS) method was used to obtain quantitative information of the amount of coating at the surface of NPs. The NPs were digested in concentrate HCl, and after that diluted by adding deionized water. The concentration of iron in the solutions was calculated using a calibration curve. The reduction of iron concentration for 1 mg of NPs was related to the amount of coatings on the Fe₃O₄ NPs. As shown in Figure 4b, Ch-Fe₃O₄ and PAA-Fe₃O₄ NPs have 12.09 and 22.66 % polymer coating on the NPs respectively. Therefore, 10.57 % of PAA-Fe₃O₄ NPs composed from PPA.

Magnetic analysis showed that the NPs have highly superparamagnetic properties, with a total magnetic saturation of 57.61 and 47.9 emu/g for Fe₃O₄ and PAA-Fe₃O₄ NPs, respectively. As can be seen in Figure 4c, there is no hysteresis loop in magnetization curves of these NPs. This indicates that NPs superparamagnetic behavior. This behavior can be observed when magnetic NPs size becomes smaller than a critical size and magnetic NPs approximately show no remanence and coercivity. This property is very important for application of magnetic NPs in biomedical fields. In the absence of magnetic fields, these NPs have no magnetic interaction with each other that prevents them from magnetic agglomeration. In presence of magnetic fields, NPs can be controlled and use in magnetic targeting. Furthermore, by applying a magnetic field with a high frequency, these NPs can be used in hyperthermia treatment. In this treatment cancer cells can be killed at around 42-45 °C [24,25].

Adsorption of biomolecules by NPs in biological environment can affect or prevent functions of NPs [26]. Moreover, it is believed that interaction between nanomaterials and proteins is the primary step to toxicity of nanomaterials [27]. Plasma protein adsorption onto surface NPs and recognition by MPS phagocytes is called opsonization. This causes that RES recognize NPs in body and remove them from blood circulation [1,16]. Moreover, thrombosis or anaphylaxis can be happened by modifying the activation of enzymatic cascades through protein adsorption [1]. For achieving longer circulation in body, NPs must have low electrostatic interaction with proteins that can be obtained via net neutral surface [18]. Furthermore, cell internalization of NPs, can be affected by protein adsorbed NPs. In the absence of protein, NPs have stronger interaction with membrane of cells and internalization can be increased. But, forming protein corona in presence of serum protein internalization reduces [21]. For achieving successful targeting, the targeting ligand on the NPs must have a more compatibility for its receptor than serum proteins. Adsorbing serum proteins onto targeting ligands on the NPs is responsible for the challenges related to in vivo NPs targeting [22]. NPs properties such as shape, size and surface chemistry influence on protein adsorption.

Protein adsorption of NPs was studied by UV-Vis spectroscopy method (Figure 5). Albumin and IgG were selected as models of protein that are two most abundant proteins in human blood plasma, respectively [10]. Coulomb interactions are very important in forming protein corona. But, these interactions are actually effective only between charges placed at the surface of NPs and proteins that are in close contact [7]. Selected proteins have different isoelectric points and charged NPs can interact with them. Isoelectric point of IgG is greater than 5.5 and can adsorb at the surface of negatively charged NPs. But, isoelectric point of albumin is less than 5.5 and can adsorb onto positively charged NPs [11]. As have showed in Figure 5, the adsorption of NPs in proteins solution is different. Generally, various interactions can occur during adsorption of protein onto NPs. these interactions include electrostatic interactions, H-bonds, van der Waals interactions, hydrophobic interactions, and $\pi - \pi$ interactions [28]. In BSA solution, PAA-Fe₃O₄ NPs with negative surface charge have the

least adsorption of albumin. But, other NPs have high positive surface charge [12], and showed higher albumin adsorption. In IgG solution result is totally different. Ch-Fe₃O₄ NPs have the highest positive surface charge and showed the lowest adsorption of IgG. In contrast, PAA-Fe₃O₄ NPs have the most IgG adsorption. About 50% of total human blood plasma mass is composed from albumin [29], and therefore, this protein is more important in plasma protein adsorption. This indicates that PAA-Fe₃O₄ NPs with lower albumin adsorption might have lower protein adsorption and longer circulation in plasma. However, these NPs have higher IgG adsorption and this can lead to some opsonization.

Using polymer coating onto NPs make them stable in water via steric stabilization. Moreover, this coating allows NPs to be used as multimodal imaging or as a nanocarrier of therapeutic agents. These can achieve by attaching other imaging contrast agent and/or drugs on the polymer functional agent or trapping them in polymer matrix. Therefore, loading of drug and release them from coating is an important parameter that can determine the efficiency of NPs for drug delivery [11]. The loading capacity and release behavior of PAA-Fe₃O₄ NPs was

studied by using ascorbic acid as a model of hydrophilic drug. PAA-Fe₃O₄ NPs were incubated in ascorbic acid solution and after separation remained drug was measured by a UV-Vis spectrophotometer at 254 nm. The drug loading contents and drug entrapment efficiency were 10% and 10.38% respectively.

Figure 6 shows the release profiles of ascorbic acid from PAA-Fe₃O₄ NPs in pH 7.4 and pH 5.8 at 37 °C. The release profiles of each pH represent continuous release up to near 40% for 50 h and then become approximately constant. The release profile indicated that release of ascorbic acid from PAA-Fe₃O₄ is not sensitive to pH of environment approximately. Drug diffusion and polymer coating degradation are two mechanisms of the release. Furthermore, drug molecules that are near the surface cause faster release in initial time [25].

Since the MRI contrast agents would eventually be used in living body, it was necessary to evaluate their toxicity.

Evaluation of toxicity of NPs is necessary to confirm that NPs are suitable for applying in drug delivery systems. Toxicity of NPs was studied on brine shrimps. 10 brine shrimps were incubated in 10 mL dispersion of NPs (1 µg/mL) and after 24 h survival brine shrimp counted. The result was showed in Figure 7 and NPs were showed good biocompatibility and represented no significant toxicity.

Conclusions

This paper describes a nanocomposition of magnetite NPs with PAA and chitosan. First, magnetite NPs synthesized by a coprecipitation method under sonication. XRD analysis showed that these NPs were synthesized successfully and magnetite NPs have good quality and purity. TEM and SEM images indicated that all NPs are in nanoscale range. Furthermore, VSM analyses confirm NPs have superparamagnetic property. Superparamagnetic behavior prevents from agglomeration of NPs in absence of magnetic field in clinical applications. FT-IR, DLS, zeta potential and AAS showed that reactions have successfully carried out. Our study showed that both

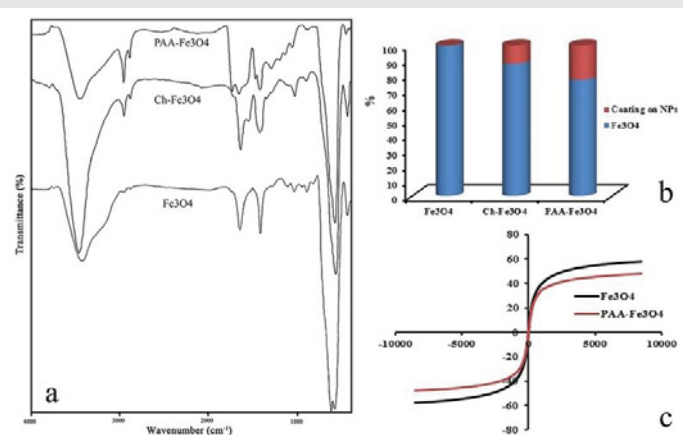


Figure 4: a) FT-IR spectra of NPs, b) AAS result for coating percent of NPs and c) Magnetization hysteresis loops of Fe₃O₄ and PAA-Fe₃O₄ NPs.

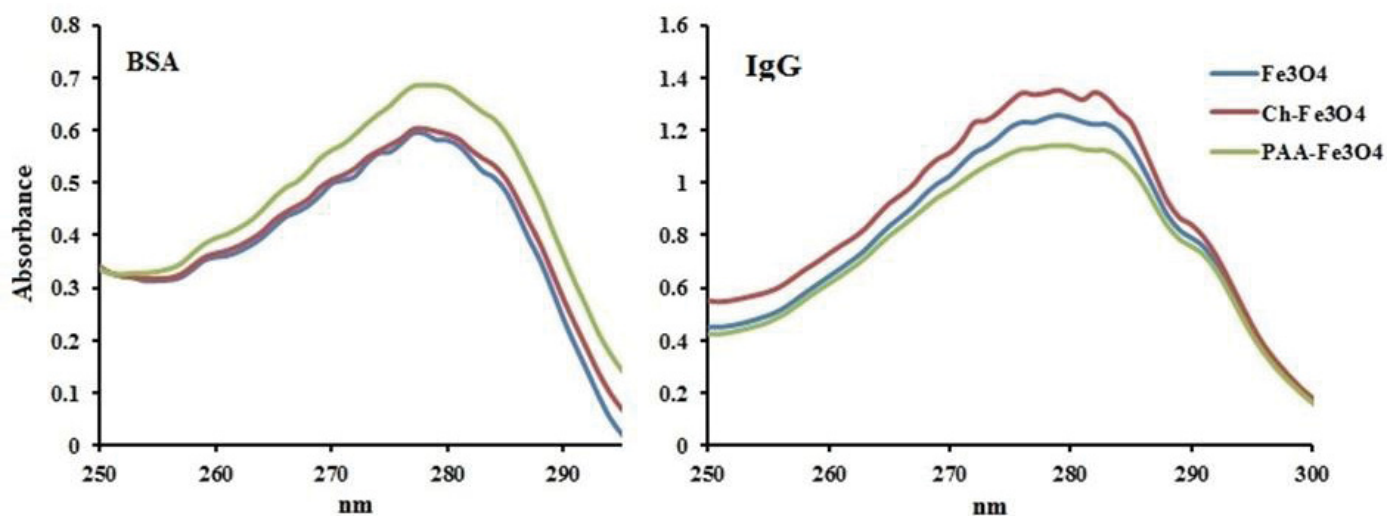


Figure 5: UV spectra of protein solutions after separation from NPs.

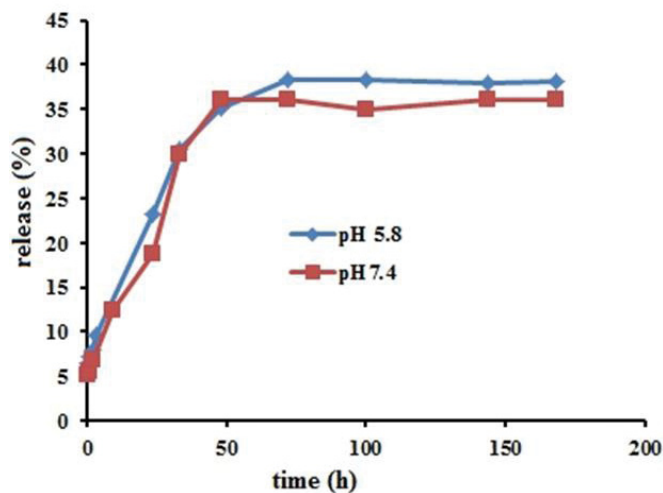


Figure 6: The release profile of ascorbic acid from PAA-Fe₃O₄ NPs.

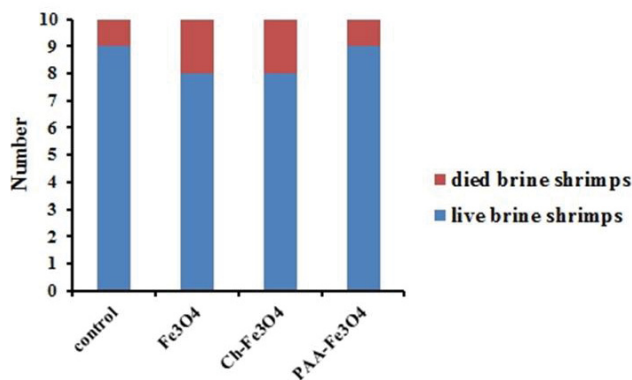


Figure 7: Live and died brine shrimps in presence of NPs.

cationic and anionic NPs could adsorb serum proteins onto their surfaces. Ch-Fe₃O₄ and PAA-Fe₃O₄ NPs have positive and negative surface charge respectively and showed different adsorption behavior in different protein medium. In albumin medium, PAA-Fe₃O₄ NPs represent the lowest adsorption because of electrostatic repulsion. But in IgG medium, these NPs showed more adsorption relative to other NPs. Albumin is the most abundant protein in plasma protein, and we can conclude that interaction with albumin is more important. This indicates that use of PAA-Fe₃O₄ NPs in biological environment represent lower opsonization. PAA-Fe₃O₄ NPs is expected to be useful as a nanocarrier for drug delivery systems and /or contrast imaging.

References

- Walkey CD, Olsen JB, Guo H, Emili A, Chan WCW (2012) Nanoparticle Size and Surface Chemistry Determine Serum Protein Adsorption and Macrophage Uptake. *J Am Chem Soc* 134: 2139-2147. [Link: https://goo.gl/sYmESV](https://goo.gl/sYmESV)
- Khoee S, Shagholani H, Abedini N (2015) Synthesis of quasi-spherical and square shaped oligoamino-ester graft-from magnetite nanoparticles: Effect of morphology and chemical structure on protein interactions. *Polymer* 56: 207-217. [Link: https://goo.gl/5PPhHi](https://goo.gl/5PPhHi)
- Ravikumar C, Bandyopadhyaya R (2011) Mechanistic Study on Magnetite

Nanoparticle Formation by Thermal Decomposition and Coprecipitation Routes. *The Journal of Physical Chemistry C* 115: 1380-1387. [Link: https://goo.gl/q22PTF](https://goo.gl/q22PTF)

- Veisoh O, Gunn JW, Zhang M (2010) Design and fabrication of magnetic nanoparticles for targeted drug delivery and imaging. *Adv Drug Deliv Rev* 62: 284-304. [Link: https://goo.gl/zFD1U7](https://goo.gl/zFD1U7)
- Yang ST, Liu Y, Wang Y-W, Cao A (2013) Proteins: Biosafety and Bioapplication of Nanomaterials by Designing Protein-Nanoparticle Interactions (Small 9-10/2013). *Small* 9: 1414. [Link: https://goo.gl/z2jKXg](https://goo.gl/z2jKXg)
- Ding D1, Wang J, Zhu Z, Li R, Wu W, et al. (2012) Tumor Accumulation, Penetration, and Antitumor Response of Cisplatin-Loaded Gelatin/Poly (acrylic acid) Nanoparticles. *ACS Appl Mater Interfaces* 4: 1838-1846. [Link: https://goo.gl/0PTnZH](https://goo.gl/0PTnZH)
- Treuel L, Brandholt S, Maffre P, Wiegele S, Shang L, et al. (2014) Impact of Protein Modification on the Protein Corona on Nanoparticles and Nanoparticle-Cell Interactions. *ACS Nano* 8: 503-513. [Link: https://goo.gl/4Ka0jZ](https://goo.gl/4Ka0jZ)
- Tenzer S, Docter D, Kuharev J, Musyanovych A, Fetz V, et al. (2013) Rapid formation of plasma protein corona critically affects nanoparticle pathophysiology. *Nat Nano* 8: 772-781. [Link: https://goo.gl/nN9miT](https://goo.gl/nN9miT)
- Hu Y, Ding Y, Ding D, Sun M, Zhang L, et al. (2007) Hollow Chitosan/Poly(acrylic acid) Nanospheres as Drug Carriers. *Biomacromolecules* 8: 1069-1076. [Link: https://goo.gl/DRCerM](https://goo.gl/DRCerM)
- Kratz F, Elsadek B (2012) Clinical impact of serum proteins on drug delivery. *J Control Release* 161: 429-445. [Link: https://goo.gl/XdYaCL](https://goo.gl/XdYaCL)
- Boyer C, Whittaker MR, Bulmus V, Liu J, Davis TP (2010) The design and utility of polymer-stabilized iron-oxide nanoparticles for nanomedicine applications. *NPG Asia Mater* 2: 23-30. [Link: https://goo.gl/BgpX5u](https://goo.gl/BgpX5u)
- Shagholani H, Ghoreishi SM, Mousazadeh M (2015) Improvement of interaction between PVA and chitosan via magnetite nanoparticles for drug delivery application. *Int J Biol Macromol* 78: 130-136. [Link: https://goo.gl/7WsM7g](https://goo.gl/7WsM7g)
- Arulvasu C, Jennifer SM, Prabhu D, Chandhirasekar D (2014) Toxicity Effect of Silver Nanoparticles in Brine Shrimp Artemia. *ScientificWorldJournal* 2014: 256919. [Link: https://goo.gl/TYYML7](https://goo.gl/TYYML7)
- Rodd AL, Creighton MA, Vaslet CA, Rangel-Mendez JR, Hurt RH, et al. (2014) Effects of Surface-Engineered Nanoparticle-Based Dispersants for Marine Oil Spills on the Model Organism Artemia franciscana. *Environ Sci Technol* 48: 6419-6427. [Link: https://goo.gl/YLT7GI](https://goo.gl/YLT7GI)
- O'Mahony JJ, Platt M, Kilinc D, Lee G (2013) Synthesis of Superparamagnetic Particles with Tunable Morphologies: The Role of Nanoparticle-Nanoparticle Interactions. *Langmuir* 29: 2546-2553. [Link: https://goo.gl/QLQgCK](https://goo.gl/QLQgCK)
- Huang C, Neoh KG, Kang E-T, Shuter B (2011) Surface modified superparamagnetic iron oxide nanoparticles (SPIONs) for high efficiency folate-receptor targeting with low uptake by macrophages. *Journal of Materials Chemistry* 21: 16094-16102. [Link: https://goo.gl/8QiEY5](https://goo.gl/8QiEY5)
- Halacheva SS, Adlam DJ, Hendow EK, Freemont TJ, Hoyland J, et al. (2014) Injectable Biocompatible and Biodegradable pH-Responsive Hollow Particle Gels Containing Poly(acrylic acid): The Effect of Copolymer Composition on Gel Properties. *Biomacromolecules* 15: 1814-1827. [Link: https://goo.gl/JizALF](https://goo.gl/JizALF)
- Liu D, Wu W, Ling J, Wen S, Gu N, et al. (2011) Effective PEGylation of Iron Oxide Nanoparticles for High Performance In Vivo Cancer Imaging. *Advanced Functional Materials* 21: 1498-1504. [Link: https://goo.gl/zZ37sC](https://goo.gl/zZ37sC)
- Saptarshi SR, Duschl A, Lopata AL (2013) Interaction of nanoparticles with proteins: relation to bio-reactivity of the nanoparticle. *Journal of Nanobiotechnology* 11: 26. [Link: https://goo.gl/ai40jS](https://goo.gl/ai40jS)

20. Hühn D, Kantner K, Geidel C, Brandholt S, De Cock I, et al. (2013) Polymer-Coated Nanoparticles Interacting with Proteins and Cells: Focusing on the Sign of the Net Charge. *ACS Nano* 7: 3253-3263. [Link: https://goo.gl/MALhHp](https://goo.gl/MALhHp)
21. Lesniak A, Fenaroli F, Monopoli MP, Åberg C, Dawson KA, et al. (2012) Effects of the Presence or Absence of a Protein Corona on Silica Nanoparticle Uptake and Impact on Cells. *ACS Nano* 6: 5845-5857. [Link: https://goo.gl/Usffo2](https://goo.gl/Usffo2)
22. Fleischer CC, Payne CK (2014) Nanoparticle–Cell Interactions: Molecular Structure of the Protein Corona and Cellular Outcomes. *Acc Chem Res* 47: 2651-2659. [Link: https://goo.gl/O35ZfJ](https://goo.gl/O35ZfJ)
23. Zhang T, Ge J, Hu Y, Yin Y (2007) A General Approach for Transferring Hydrophobic Nanocrystals into Water. *Nano Lett* 7: 3203-3207. [Link: https://goo.gl/Wt6HOz](https://goo.gl/Wt6HOz)
24. Patra S, Roy E, Karfa P, Kumar S, Madhuri R, Sharma PK (2015) Dual-Responsive Polymer Coated Superparamagnetic Nanoparticle for Targeted Drug Delivery and Hyperthermia Treatment. *ACS Appl Mater Interfaces* 7: 9235-9246. [Link: https://goo.gl/RFreG8](https://goo.gl/RFreG8)
25. Wu Y, Guo J, Yang W, Wang C, Fu S (2006) Preparation and characterization of chitosan–poly(acrylic acid) polymer magnetic microspheres. *Polymer* 47: 5287-5294. [Link: https://goo.gl/liuJr](https://goo.gl/liuJr)
26. Ashby J, Schachermeyer S, Pan S, Zhong W (2013) Dissociation-Based Screening of Nanoparticle–Protein Interaction via Flow Field-Flow Fractionation. *Analytical Chemistry* 85: 7494-7501. [Link: https://goo.gl/suUDLF](https://goo.gl/suUDLF)
27. Zuo G, Kang S-g, Xiu P, Zhao Y, Zhou R (2013) Interactions Between Proteins and Carbon-Based Nanoparticles: Exploring the Origin of Nanotoxicity at the Molecular Level. *Small* 9: 1546-1556. [Link: https://goo.gl/oSkvGs](https://goo.gl/oSkvGs)
28. Yang ST, Liu Y, Wang YW, Cao A (2013) Biosafety and Bioapplication of Nanomaterials by Designing Protein–Nanoparticle Interactions. *Small* 9: 1635-1653. [Link: https://goo.gl/wWtgti](https://goo.gl/wWtgti)
29. Nair LS, Laurencin CT (2007) Biodegradable polymers as biomaterials. *Progress in Polymer Science* 32: 762-798. [Link: https://goo.gl/4ikjxz](https://goo.gl/4ikjxz)